Available online at www.sciencedirect.com
ScienceDirect
Journal of Power Sources 173 (2007) 200–209
JOURNAL OF POWER SOURCES
www.elsevier.com/locate/jpowsour

Review

Bio-ethanol, a suitable fuel to produce hydrogen for a molten carbonate fuel cell

Francesco Frusteri *, Salvatore Freni

Institute, CNR-ITAE "Nicola Giordano", Via S. Lucia sopra Contesse 5, I-98126 Messina, Italy

Received 7 September 2006; received in revised form 12 April 2007; accepted 29 April 2007
Available online 5 May 2007

Abstract

Catalytic and technological aspects in the use of bio-ethanol as fuel to produce hydrogen in both internal (IR-MCFC) and indirect internal reforming (IIR-MCFC) configurations have been considered. In MCFC conditions, even operating at total ethanol conversion, hydrogen productivity depends on the catalyst efficiency to convert methane formed through a mechanism, which foresees as first step the dehydrogenation of ethanol to acetaldehyde and as a second step the decomposition of acetaldehyde to CO and CH_4. Potassium doped Ni/MgO, Ni/La_2O_3 and Rh/MgO resulted to be the most promising catalysts to be used for the hydrogen production by steam reforming of bio-ethanol. Coke formation represents a serious problem, however, it can be drastically depressed by adding to the reaction stream a low amount of oxygen.

On the basis of catalytic and technological evaluations, indirect internal reforming configuration should be the more suitable to operate with bio-ethanol. MCFC electric performance using a hydrogen rich gas coming from steam reforming of bio-ethanol is very similar to that of MCFC fed with pure hydrogen. However, the high content of steam in the flow reaction stream must be careful computed for a good thermal balance of the overall plant.

Keywords: MCFC; Technological aspects; Bio-ethanol steam reforming; H_2 production

Contents

1. Introduction 200
2. Working principle of MCFC 201
3. Thermodynamic and cell dynamics evaluations 202
4. Thermal balance of IR-MCFC fed by ethanol 202
5. Technological aspects 203
6. Catalytic aspects 205
   6.1. Ethanol steam reforming at low temperature 206
   6.2. Ethanol steam reforming at high temperature 206
7. Conclusions 209
   References 209

1. Introduction

High temperature fuel cells (MCFC, SOFC) are promising systems to co-generate heat and electricity with high efficiency. In case of molten carbonate fuel cell (MCFC) it is very important to evaluate the thermal balance of the stack to design a system characterized by high yield. Although natural gas is the most investigated fuel, the MCFC can be fed by a wide variety of fuels. Here, the possibility to use the heat generated at electrodes to produce hydrogen by ethanol reforming processes has been considered. Indirect and direct internal reforming configurations were evaluated either in terms of heat and mass transfer

* Corresponding author. Tel.: +39 090624233; fax: +39 090624247.
E-mail address: francesco.frusteri@itae.cnr.it (F. Frusteri).

0378-7753/$ – see front matter © 2007 Elsevier B.V. All rights reserved.
doi:10.1016/j.jpowsour.2007.04.065

phenomena or in terms of compatibility of catalyst with cell components.

2. Working principle of MCFC

As well known, the fuel required by the MCFC consists of a hydrogen rich gas mixture like hydrocarbon reformed gas. The working temperature for MCFC is around 923 K and the cell releases heat when produces electricity. A such peculiar condition makes possible the integration of the electrochemical cell section with the fuel reformer reactor in order to design high thermal efficiency system. This concept is called as "internal reforming" (IR) and can be realized by two different geometric configurations defined as "direct internal reforming" (DIR) and indirect internal reforming (IIR). The first configuration is based on a thermo-chemical integration between reformer and cell anode module. In this case the reforming reaction will produce hydrogen which is immediately consumed by electro catalytic cell reaction, furthermore, the heat generated by hydrogen oxidation is directly used for the reforming process since there is no physical barrier between reformer and anode catalyst. In addition the reforming process equilibrium will take advantage from the fact that hydrogen is consumed when produced. In Fig. 1 is schematically represented the MCFC operating with direct internal reforming configuration.

In the indirect internal reforming configuration, the reforming catalyst is placed into a cell metallic hardware but it is physically separated from anode compartment. In this geometry, the equilibrium of reforming process is not influenced by hydrogen consumption, but the contact between electrolyte vapours and reforming catalyst is avoided. The scheme of IIR-MCFC is shown in Fig. 2.

The direct or indirect internal reforming configurations affect the thermal efficiency of the system, but they do not influence the semi-reactions of electrodes that remain:

$$\text{to the anode}: \ H_2 + CO_3^{2-} \rightarrow H_2O + CO_2 + 2e^-$$

$$CO + CO_3^{2-} \rightarrow 2CO_2 + 2e^-$$

$$\text{and to the cathode}: \ O_2 + 2CO_2 + 4e^- \rightarrow 2CO_3^{2-}$$

that can be expressed by the following overall reaction:

$$H_2 + CO_2 + \tfrac{1}{2}O_2 \rightarrow H_2O + CO_2$$

From the analysis of the overall reaction, it is evident that CO_2 balance is neutral. In fact, CO_2 is produced by the anode semi-reaction and consumed by the cathode semi-reaction. This is possible by recycling CO_2 from anode exhaust to cathode inlet. Thus, a MCFC plant lay-out will be provided with an external combustor, where unreacted fuel (exhaust anode outlet gas) will be burned and recycled to cathode inlet. This technical solution makes the MCFC system able to produce electricity and steam at high temperature (923 K). The production of heat is directly correlated to the current density and it is so large to require a stack cooling system to avoid the overheating risk. The coupling of endothermic reactor (like reformer) to the cell can enhance the thermal balance in the system and this is the goal of internal reforming configurations.

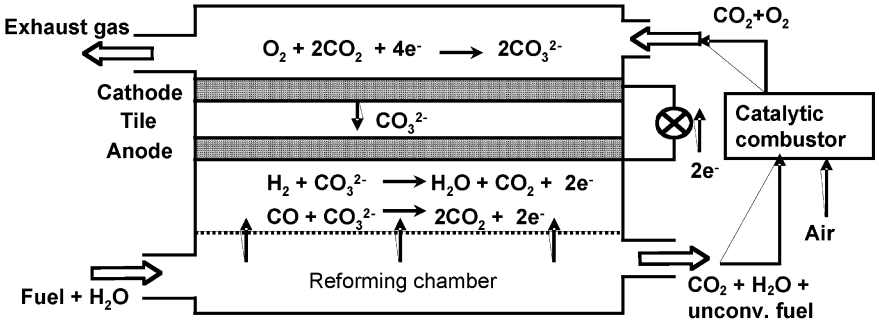

Fig. 1. MCFC system: direct internal reforming configuration.

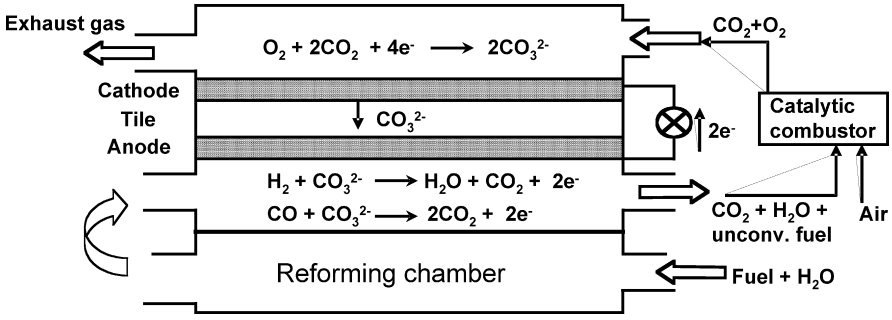

Fig. 2. MCFC system: indirect internal reforming configuration.

3. Thermodynamic and cell dynamics evaluations

If we consider that ethanol steam reforming proceeds according to the following scheme [1]:

$$C_2H_5OH + H_2O \rightleftharpoons 4H_2 + 2CO \quad (1)$$

$$CO + H_2O \rightleftharpoons H_2 + CO_2 \quad (2)$$

$$CO + 3H_2 \rightleftharpoons CH_4 + H_2O \quad (3)$$

the thermodynamic equilibrium constants K_1, K_2 and K_3 can be expressed by the following equations:

$$K_1 = \frac{x_{CO}^2 x_{H_2}^4}{x_{EtOH} x_{H_2O}} P^4 \quad (4)$$

$$K_2 = \frac{x_{CO_2} x_{H_2}}{x_{CO} x_{H_2O}} \quad (5)$$

$$K_3 = \frac{x_{CH_4} x_{H_2O}}{x_{CO} x_{H_2}^3} P^{-2} \quad (6)$$

where x_i is the component molar fraction and P is the overall reaction pressure.

As well known, the equilibrium composition of each product can be determined if we consider the non-linear equations system comprising the equilibrium constants relationship and the mass balance corresponding to the above reported process reactions. The simplest way to solve such a system consists in the compilation of a mathematical model based on iterative process. Thus, starting from initial values for reaction conversions and for equilibrium constants, a multi-dimensional convergent method should be able to solve the system.

The outlet gas composition, through gas partial pressures, will affect directly the cell Nernst's potential, given by:

$$V = V_0 + \frac{RT}{2F} \ln \frac{[P_{H_2} P_{O_2}^{1/2} P_{CO_2(c)}]}{[P_{H_2O} P_{CO_2(a)}]} \quad (7)$$

where V_o is the standard potential of cell reactions, P the partial pressure of gases, R the universal gas constant (8.314 J K^{-1} mol) and F is the Faraday's constant (96487 C/g-eq).

Further, the fuel cell is affected by irreversible potential losses due to electrodes over-potentials and ohmic resistance of the cell components. Thus, the working cell voltage, V_{eff}, can be determined by the following relationship [2]:

$$V_{eff} = V - (\mu_a + \mu_c) - IR_i S_o \quad (8)$$

where μ_a and μ_c are the anode and cathode over-potentials, I the current density, R_i the specific ohmic cell resistance and S_o is the effective electrodes surface.

As regard to the overall energy balance, it should take into account both the inlet and the outlet contributions, than the inlet energy (fuel + oxidant) must be equal to the outlet energy (electricity plus recovered heat plus lost heat) and can be expressed as follow [3]:

$$m_f h_f + m_o h_o = W + Q_u + \sum_w Q_w + \sum_w m_w h_w \quad (9)$$

Table 1
EtOH steam reforming: outlet gas stream composition

	H_2	CO_2	H_2O	C_2H_5OH	CH_4	CO
Out Composition (%)	30.10	7.50	56.52	0	1.69	4.19
Selectivity (%)	–	56.07	–	–	12.66	31.27
Conversion (%)	–	–	–	100	–	–

Test conditions: $T_R = 923$ K; $P = 0.16$ MPa; $H_2O/C_2H_5OH = 8.4$ mol vol^{-1}; GHSV = 37,500 h^{-1}; catalyst = 5% Rh/Al_2O_3.

where m is the mass, h the enthalpy, W the electric energy released by the cell, Q the heat exchanged while the index f, o, u, w are referred to fuel, oxidant, useful fraction and wasted fraction.

The efficiency of the transformation process from heat to electricity can be determined by the following expression:

$$\eta = \frac{W}{m_f h_f} \quad (10)$$

In case bio-ethanol is used as a fuel in MCFC, on the basis of thermodynamic considerations, at 650 °C a full ethanol conversion can be expected. Considering that bio-ethanol is a diluted mixture (11–12 vol% of ethanol in water), the high steam/carbon ratio will makes unfavorable conditions for methane and carbon monoxide formation and contributes to remove coke, while in the meantime enhances hydrogen production and ethanol decomposition [4]. To confirm such assertion, in Table 1, as example, the outlet gas composition detected in the process of bio-ethanol steam reforming is reported [1].

Notwithstanding the large presence of steam, coming also from electrochemical reaction, the Nernst potential determined for a MCFC, fed to the anode with reformed bio-ethanol gas and to the cathode with air and CO_2 mixture (80 and 20%, respectively), results to be equal to 1151 mV ($V_o = 1021$ mV). This value does not significantly differ from that expected for a MCFC fed by syngas coming from a conventional hydrocarbon reforming process.

In terms of thermal balance, in case of bio-ethanol use, the high flow rate of steam in the outlet flow stream must be careful computed, in fact, a lot of heat is required for water vapourization and the design of the plant should comprise a system to recover the latent heat of exhaust steam released at MCFC anode side.

4. Thermal balance of IR-MCFC fed by ethanol

The heat balance of an MCFC with internal reforming (IR-MCFC) appears to be complex if compared to a conventional molten carbonate fuel cell. In fact, the overall energy production is the resultant of several contributions, among them the most important is the electricity, but if only the heat flux will be taken into account, it appears that the overall thermal balance is a function of the cell current density. For a MCFC, two different zones exist: one, where the endothermicity of reforming is prevailing and the heat must be supplied from an external source (zone characterized by low current density); another one, where the electrochemical cell reaction takes place producing the heat which

Table 2
DIR-MCFC fed with ethanol/water mixture: working conditions

Temperature (K)	923
Pressure (bar)	1.0
Specific cell resistance ($\Omega\,cm^{-2}$)	0.75
Inlet flow of ethanol ($ml\,h^{-1}\,cm^{-2}$)	41.87
H_2O/EtOH ($mol\,mol^{-1}$)	3.0
Cathode inlet flow ($ml\,h^{-1}\,cm^{-2}$)	590
Cathode inlet flow composition (%)	80 air + 20 CO_2
Oxidant utilization (%)	35 at 0.15 A cm^{-2}

could be used to sustain the endothermic reforming reaction.

In the IR-MCFC, the heat balance is strictly depending upon current density. Then, in practice, to sustain the endothermic steam reforming process a minimum value of current density is required. As example, for a IR-MCFC system, working at operative conditions reported in Table 2, the minimum current density required to reach the thermal equilibrium corresponds to 114 mA cm^{-2} as also shown in Fig. 3. For large power MCFC plant integrated with a cogeneration system the heat balance can be evaluated as follow [5]:

$$Q_{cell} + Q_X - Q_{ref} + (Q_{A\,in} - Q_{A\,out}) + (Q_{C\,in} - Q_{C\,out}) - Q_W + Q_{EXT} = 0 \quad (11)$$

$$Q_{cell} = Q_{react} - Q_E$$

Q_{react} is the electrochemical energy of cell reaction given by: $\Delta H\, X_{h2}$, ΔH the enthalpy of water formation reaction; X_{h2} the flow of converted hydrogen, Q_E the electric energy released by the system, Q_X the heat generated by direct reaction of cross-over reactans, Q_{ref} the heat required for steam reforming process, $(Q_{A\,in} - Q_{A\,out})$ the heat due to the difference between heat content of inlet and outlet anode gases, $(Q_{C\,in} - Q_{C\,out})$ the heat due to the difference between heat content of inlet and outlet cathode gases, Q_w the heat lost by thermal radiation and Q_{EXT} is the heat exchanged with external sub-system devices.

It can be seen from Eq. (11) that to careful evaluate the overall heat balance of a MCFC stack it is need to take into consideration also: (i) the heat of combustion released by direct oxidation of hydrogen diffused by cross-over, Q_X; (ii) the heat lost by thermal radiation, Q_w and (iii) the heat exchanged with external sub-system devices, Q_{EXT}.

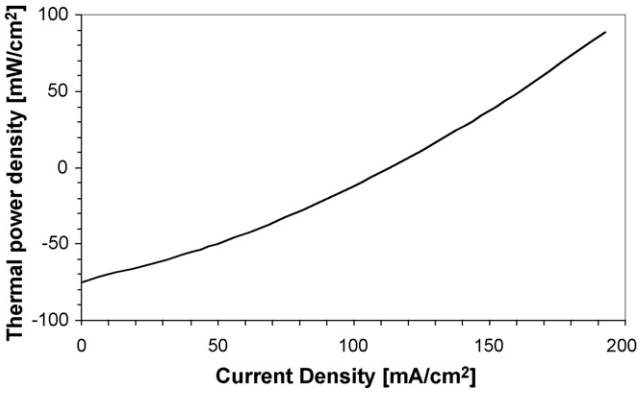

Fig. 3. Thermal power density as a function of current density.

5. Technological aspects

The steam reforming is an endothermic process and when it is coupled to a MCFC, that as well known, is an isothermal process, the overall thermal balance enhances as well as the thermal integration is efficient. But, such an integration implies that anode fuel composition is depending by the thermodynamic equilibrium of reforming process. So, temperature, pressure and current density will be the operative parameters that can influence such a composition and consequentially, the MCFC system's performance.

Some authors have studied [6–8] the variations of equilibrated gas composition as a function of pressure (0.1–0.5 MPa) and temperature (873–973 K) into a wide range typical of MCFC operative conditions. Test conditions taken into account by the authors are slightly different from that expected by using bio-ethanol, in fact, they adopted an H_2O/EtOH ratio equal 2.0 against 8.4 that is the typical one for bio-ethanol/water mixture. However, this difference should not invalidate the approach followed to evaluate the influence of the operative parameters (temperature and pressure) on the overall process.

The influence of temperature appears to be very significant on both reformer and cell performance. Thus, when the system (reformer plus MCFC) will operate at low temperature (less than 923 K) a drop of cell voltage must be expected due to: (i) the lowering of hydrogen yield (because lower temperature means poorer reformer performance); (ii) the increasing of cell ohmic losses (poorer electrolyte conductibility) and electrode polarizations (slower kinetic of electro catalytic reactions).

Quite negligible appears to be the influence of the pressure on the cell performance. In this case, a variation of this parameter influences two different mechanism. In fact, higher values of pressure will inhibit the hydrogen production with a drop of reformer performance but, in the meantime, it will enhance the hydrogen partial pressure and consequently also the electrochemical cell reaction will be favored. On the whole, these two mechanisms will produce two opposite effects whose global resultant is nearly negligible. It has been demonstrated that a complete conversion of ethanol can be expected if H_2O/EtOH ratio above 2 is used, independently from the selected system configuration (IIR or DIR).

As example, the hydrogen concentration (see Fig. 4a and b) for DIR-MCFC supplied by a mixture of H_2O/EtOH = 2 and flow rate of EtOH corresponding to a 75% of hydrogen utilization at a current density of 190 mA cm^{-2}, changes with reformer temperature (from 58.9% at 973 K and 0.1 MPa, to 46.8% at 873 K and 0.1 MPa), pressure (see Fig. 4b) and cell current density (when is $I = 0$, only reformer parameters will influence the hydrogen concentration). Further, these operative conditions influence the global gas compositions through formation of CO and CH_4. In Fig. 5, the gas composition versus current density for a MCFC integrated directly with an ethanol reformer is shown, the expected concentration of methane and carbon monoxide at anode is 8 and 17%, respectively.

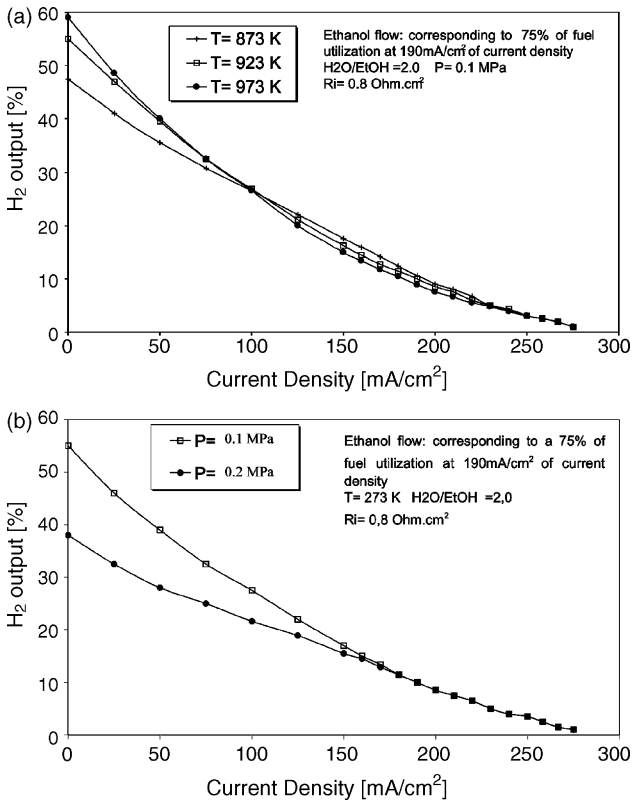

Fig. 4. (a) Hydrogen concentration on anode gas composition vs. current density at $P = 0.1$ MPa and $T = 873$–973 K for EtOH DIR-MCFC, (b) hydrogen concentration on anode gas composition vs. current density at $T = 923$ K and $P = 0.1$–0.5 MPa for EtOH DIR-MCFC.

As above-mentioned, the configuration of direct internal reforming represents the best solution to integrate reformer and cell sub modules, but it exists a severe problem due to the physical interaction between electrolyte vapours and reforming catalyst that makes such application quite critical [9,10]. On this order, some authors [11] studied the possibility to solve this problem by insertion of porous membranes into anode compartment to protect internal reforming catalyst. But, in this case, the reforming step must be performed at high pressure in order to have enough hydrogen flux permeation through the membrane structure and, thus, to have enough supplying of hydrogen to the

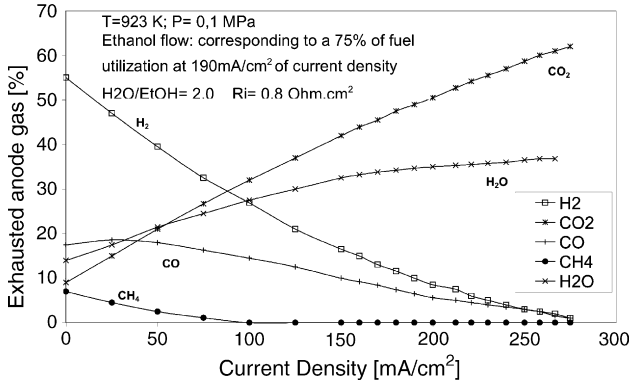

Fig. 5. Outlet anode gas composition vs. current density at 973 K and 0.1 MPa for EtOH DIR-MCFC.

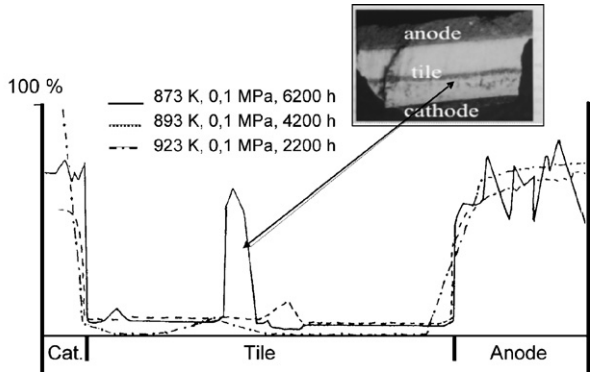

Fig. 6. Ni distribution along cross section of ER-MCFC for different operative temperature and operational time.

anode. The system complexity of this configuration makes very difficult its concrete application.

Otherwise, the indirect internal reforming configuration is considered a good compromise to have a good thermal integration between reformer and electrochemical sub-modules and to protect the catalyst from poisoning by alkali vapours.

Usually, MCFC balance plant is designed for having a partial recycling of outlet anode gas flow to the inlet cathode side in order to supply the carbon dioxide needed to cathode semi-reaction. Extremely attention must be paid on the determination of the flow rate of carbon dioxide which must be recycled because high partial pressure of CO_2 on cathode side will dramatically accelerate the dissolution of the electrode. The basic material (pre-lithiated NiO) of the cathode structure tends to react with the recycled CO_2 to form Ni ions that have a slightly solubility in the electrolyte melt. Due to this solubility, the Ni^{2+} ions migrate by the electrolyte melt, toward anode side where they are reduced to metallic Ni by the hydrogen diffused into the melt. This process is slow but constant in the time and produces the cathode destruction and the formation of a thick layer of metallic nickel in the middle of the electrolyte tile cross section [12,13]. The distribution of Ni particles detected into the cross sections of MCFC, operating at three different temperatures, is shown in Fig. 6. The mechanism of NiO dissolution is a function of the acidic/basic properties of the carbonates melt. In general, a melt of carbonates tends to be dissociated into its acidic and basic compounds:

$$M_2CO_3 \leftrightarrow M_2O + CO_2 \quad \text{(I)}$$

where, M_2O acts as base by supplying O^{2-} ions

$$M_2O \leftrightarrow 2M^+ + O^{2-} \quad \text{(II)}$$

and CO_2 respect to the acidic component:

$$CO_2 + O^{2-} \leftrightarrow {CO_3}^{2-} \quad \text{(III)}$$

The NiO in contact with carbonates melt can be involved into two different chemical reaction mechanisms. The first is called “acidic dissolution” and it is expressed by the following reaction:

$$NiO \leftrightarrow Ni^{2+} + O^{2-} \quad \text{(IV)}$$

(this is the preferential pathway of NiO dissolution when the activity of O^{2-} ions activity is very low) and the second mechanism is called "basic dissociation" and the reactions involved are:

$$NiO + O^{2-} \leftrightarrow NiO_2^{2-}$$

$$2NiO + O^{2-} + \tfrac{1}{2}O_2 \leftrightarrow 2NiO_2^{2-}$$

With regard to MCFC, working at 923 K and 0.1 MPa with a eutectic mixture of lithium and potassium carbonates, the experimental evidences have indicated that the NiO acidic dissolution is the prevailing mechanism of cathode deterioration. From a general point of view, for MCFC, this mechanism is influenced by the basicity of electrolyte melt, by the CO_2 partial pressure in the cathode inlet flow and by temperature. The basic properties of the electrolyte can be improved if K_2CO_3 (more acidic that Li_2CO_3) will be substituted with more basic carbonate, like Na_2CO_3, even if this choice can require additional investigations about segregation problems that can arise for long-term operations. The CO_2 partial pressure value influences directly the rate of NiO solubility on the carbonate melt. CO_2 is needed on cathode side because it is involved in the electrode semi-reaction and a poor CO_2 content will produce high polarization losses. But high CO_2 partial pressure enhances dramatically NiO dissolution process, thus, the choice of CO_2 concentration on inlet cathode flow must not exceed 25–30% at 923 K and 0.1 MPa. At last, the temperature influences the basicity of a molten carbonate mixture and then the rate of cathode dissolution [14]. In fact, with respect to the acidic dissolution, the influence of the temperature can be explained by taking into account the carbonates decomposition reaction:

$$CO_{(l)3}^{2-} \rightarrow O_{(l)}^{2-} + CO_{2(g)} \quad (V)$$

When temperature decreases, carbonate dissolution is greatly un-favored and this produces a global lower of O^{2-} activity (due to the increase of melt acidity) with a consequent shift of reaction (IV) towards right side with an overall promotion of NiO acid dissolution. This statement has been confirmed by experimental evidences, in fact, as reported in Fig. 6, a MCFC operating at 873 K (versus 923 K as usual operating temperature) for relatively short time (6200 h) showed a massive deposition of dissolved Ni in the middle cross section of the tile.

6. Catalytic aspects

Steam reforming is a well-established industrial process for the production of hydrogen or syngas from natural gas, other hydrocarbons and alcohols. In particular, steam reforming of methane is highly endothermic ($\Delta H = 206\,kJ\,mol^{-1}$) and the large scale industrial process is usually carried out above 700 °C and low pressure to ensure high methane conversion and then high hydrogen production. In case of alcohol, for example methanol, since alcohols are much more reactive than methane, the reaction can be carried out at lower temperature (for example methanol can be reformed at 250 °C over Cu based catalysts). Even ethanol could be steam reformed at low temperature

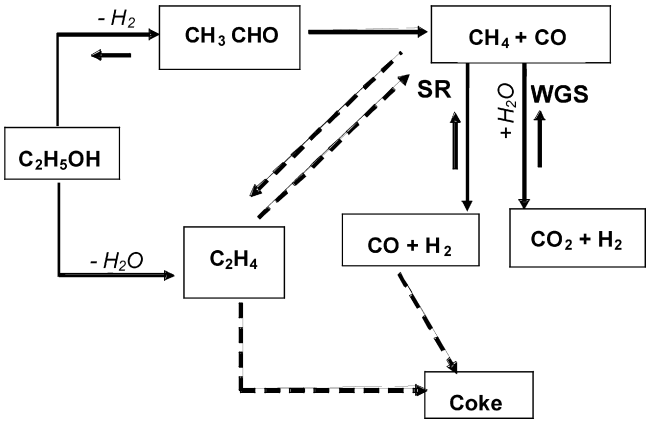

Fig. 7. Steam reforming of ethanol: reaction mechanism scheme.

(250–300 °C) but unfortunately even if it is possible to operate at total ethanol conversion, hydrogen productivity is usually low due to the formation of side products like acetaldehyde and methane.

To better understand such last assertion, it is necessary to refer to the reaction mechanism recently proposed by different authors [15–18] (see Fig. 7). Ethanol, in the presence of transition metals usually utilized as active catalyst to perform steam reforming processes, is firstly dehydrogenated to acetaldehyde [16]. Further to consider the possibility to obtain syngas directly from acetaldehyde ($CH_3CHO + H_2O = 2CO + 3H_2$), since acetaldehyde is not so stable, its tends to decompose in CH_4 and CO. This step is crucial, since if acetaldehyde evolves towards the formation of methane, the hydrogen productivity is linked to the methane conversion obtainable by steam reforming reactions only. Then, according to the thermodynamic equilibrium prevision (see Fig. 8) to obtain high methane conversion, temperatures higher than 800 °C are required.

From the discussion above reported it clearly emerge that hydrogen production by steam reforming of ethanol, notwithstanding ethanol is a very reactive molecule, could in many cases controlled by methane steam reforming and water gas shift reactions. Naturally, this means that catalytic systems adequate to perform steam reforming of ethanol should possess physical–chemical properties similar to that used for conven-

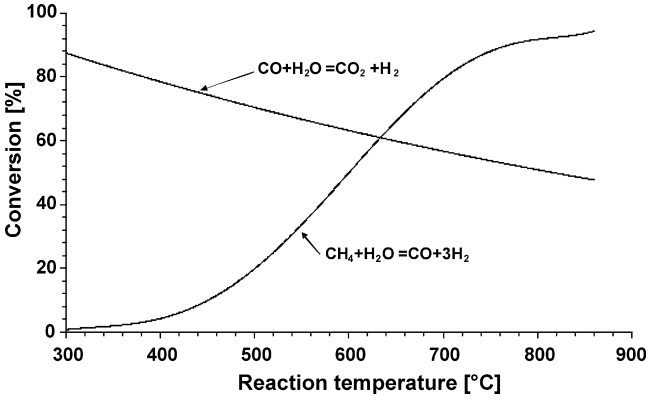

Fig. 8. Thermodynamic conversion values of CH_4 steam reforming and water gas shift reactions.

tional methane steam reforming process, but they must operate with the disadvantage to be in contact with a organic molecule like ethanol that at high temperature can easily decompose. A further complication arising from the use of ethanol regard the possibility that its may be dehydrated to ethylene, and this as well known, is a big problem since ethylene is a well known coke formation promoter.

Several papers have been published in the last decade both considering the possibility to produce hydrogen from bio-ethanol at low or high temperatures. In the following paragraphs, both approaches are considered.

6.1. Ethanol steam reforming at low temperature

In recent years, several papers have been published to evaluate the possibility to produce hydrogen from bio-ethanol at low reaction temperature. Even though it is not easy to rationalize results obtained in different labs and then in different reaction conditions, an effort has been done addressing the attention to evaluate how physical–chemical properties of catalyst can affect reaction pathway.

Cobalt has been largely investigated and proposed as appropriate metal to promotes the production of CO free hydrogen [19–24]. The influence of support properties on activity, stability and product distribution of Co supported on MgO, Al_2O_3, SiO_2, TiO_2, V_2O_5, ZnO, La_2O_3, CeO_2 and Sm_2O_3 has been evaluated [19]. On acidic carriers mainly of alumina, even operating at high ethanol conversion significant amount of ethylene was formed while on basic carriers acetaldehyde was prevalent. Co/ZnO catalyst resulted to be the most promising one, low amount of CO was detected and H_2 and CO_2 selectivity of 71.3 and 20.2% where obtained, respectively [20]. However, even on such promising system CH_4, C_2H_4, C_3H_6, CH_3CHO and Me_2CO were detected confirming that reaction evolves with a complex mechanism and by operating at relatively low reaction temperature (<400 °C) the obtainment of pure hydrogen is really a challenge. The same authors have recently evaluated the effect of sodium as promoter of Co/ZnO catalyst concluding that sodium enhance activity and stability mainly depressing coke formation, furthermore only a small amount of methane was detected as side product [21]. Other papers devoted to the study of Co supported catalysts revealed that deactivation due to the coke formation and methane production represent problems, which are not easy to overcome [22].

The possibility to use Ni as active metal has been largely considered [23–29]. The behaviour of Ni/Y_2O_3, Ni/La_2O_3 and Ni/Al_2O_3 has been evaluated by operating at reaction temperature ranging from 250 to 350 °C [23]. Even though on all catalytic systems investigated it is possible to operate at ethanol conversion very close to 100%, too high methane selectivity (20–30%) were observed. By comparing such results with those obtained on Co catalysts seems clear that Ni works with a different mechanism promoting the formation of methane through dehydrogenation of ethanol to acetaldehyde followed by the decomposition of acetaldehyde to CO and CH_4. The addition of Cu [24–26] seams to depress methane formation but probably negatively affects Ni reforming activity since high acetaldehyde selectivity (>40%) was observed.

The influence of Ce/Zr ratio on the redox behaviour of Ni in a series of NiO-CeO_2-ZrO_2 catalysts was investigated [27]. The catalysts exhibited good catalytic activity and stability (endurance test of 500 h was performed) but even in such case methane selectivity higher than 6–7% have been obtained. The reaction of ethanol over noble metals has also been considered since noble metals are known to be very active in activation of the carbon–carbon bond [28–31]. Rh-Pt/CeO_2 [28], Pd/C [29] and Pd/Al_2O_3 [30] have been investigated and as expected they work with high ethanol conversion rates, but high CH_4 and acetaldehyde selectivity in case of Rh and Pd, respectively, has limited the obtainment of high hydrogen productivity.

6.2. Ethanol steam reforming at high temperature

Taking into account that MCFC is a co-generative system operating at 650 °C high temperature ethanol steam reforming process is attractive because it offers the possibility to be directly coupled with a MCFC system utilizing the heat generated at electrode to produce hydrogen. Naturally, as previously described, further to consider the problem linked to the deactivation of catalyst caused by the presence of alkali carbonate originating from electrolyte, the high reactivity of ethanol and the presence of high partial pressure of water vapour in case of use of bio-ethanol represent furthers complications for the design of an appropriate catalyst for such purpose.

Ni based catalysts have been largely investigated [31] but also Co and noble metal catalysts, mainly Rh, have been studied. Results obtained over Ni catalysts supported on La_2O_3, Al_2O_3, YSZ and MgO [32] revealed the fundamental role exerted by La_2O_3 in stabilizing the catalyst activity by decorating the Ni particles with a thin film of lanthanum oxycarbonate species, which acts as a cleaner of metallic surface of carbon deposits ($La_2O_2CO_3 + C \rightarrow La_2O_3 + 2CO$). At 650 °C and $H_2O/C = 3$ Ni/La_2O_3 catalyst resulted to be the most stable and active system but hydrogen selectivity lower than 77% was obtained due to the formation of appreciable amounts of CH_3CHO and CH_4.

Steam reforming of bio-ethanol, in simulated MCFC operative conditions ($H_2O/C = 4.2$, $T_R = 650$ °C) was investigated over MgO supported Ni, Co, Pd and Rh catalysts [16]. The use of a basic carrier such as MgO allowed to work with modest coke formation. The advantages gained are attributable to the inhibition of the ethanol dehydration reaction (ethylene production) and to the electronic enrichment of supported metal which contribute to depress the Boudouard reaction ($2CO \rightarrow C + CO_2$). Endurance test of 650 h performed at 10,000 h^{-1} revealed a good performance of Ni/MgO which worked at total ethanol conversion with a H_2 selectivity higher than 96% [4]. The addition of alkali (Li, K) stabilizes the Ni/MgO catalyst system mainly by depressing the metal sintering [33]. Authors have reported that Ni particle size (d*s*) affects the TOF: higher TOF for higher d*s*. The structure-sensitive character of the ethanol dehydrogenation reaction was invoked to explain such result.

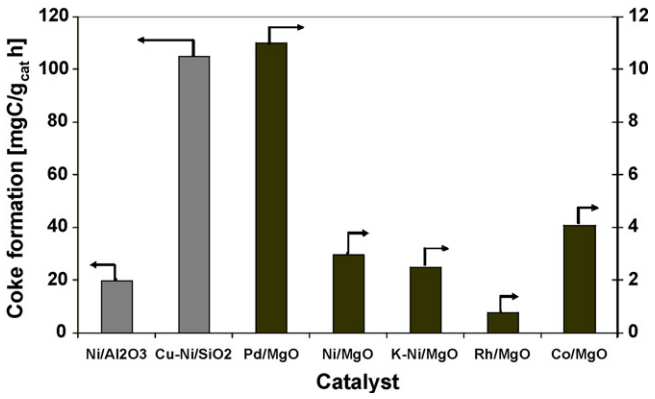

Fig. 9. Coke formation over different supported catalysts.

In general, what emerge from literature data available is that steam reforming of bio-ethanol at high temperature is mainly affected by metal sintering, very probably due to the presence of large amount of water, and coke formation caused by the low thermal stability of ethanol, which easily decompose and to the formation of ethylene by dehydration reaction. Notwithstanding several papers have been published, only a few data concerning the coke formation were reported [16,22,34]. In Fig. 9, a comparison of literature data in terms of coke formation rate over different catalysts is reported. It can be observed that catalysts based on the use of acidic carriers like alumina and silica are affected by the formation of huge amount of coke since acidic sites promote dehydration of ethanol to ethylene.

However, the kinetic of coke formation is not depending upon the support nature only, but also from the nature of active metal. In particular, on Pd/MgO higher coke formation rate respect to Ni/MgO were observed, while on Rh/Al_2O_3, in spite of the presence of alumina coke forms with very low rate.

As regard, the morphology of carbon formed during reaction, further to depend upon the reaction condition used, a fundamental role was played also by the nature of both support and metal and from their chemical–physical interaction. TEM overview of both used bare and alkali doped Ni/MgO catalysts (see Fig. 10) revealed the formation of both filamentous and condensed carbon. In general terms it seems that a relationship exist between the size of carbon filament and the Ni particle size: the higher is the Ni particle size the higher is the size of carbon filaments.

As reported in the current literature, in case of methane reforming on Ni based catalysts, it is well known that methane decomposes on the exposed surface of the metal particle releasing hydrogen and carbon which tends to dissolve in the metal particle. Naturally, the solubility of carbon in a metal depends upon several factors. For example, due to the exothermic decomposition of methane, it is believed that a temperature gradient exists across the catalyst particle. Since the solubility of carbon in a metal is temperature dependent, precipitation of excess carbon will occur at the colder zone behind the particle, thus, allowing the solid filament to grow with the same diameter as the width of the catalyst particle [35]. Further to consider the effect of temperature, the carbon diffusion through the Ni particle depends upon: (i) thickness of particle (effective length of carbon diffusion); (ii) metal specific surface area; (iii) concentration of carbon in metal at the gas side and (iv) concentration of carbon at the rare side of metal particle [36]. As a consequence, it can be inferred that the carbon formation is directly proportional to the driving force of diffusion. At steady state, the coking rate equals the rate of carbon diffusion through the metal particles. It was evident from literature that metal particle size plays a crucial role in the kinetic coke formation independent of the carrier used to support the active metal. The benefit of using of K doped catalyst (see Fig. 10b) to avoid the formation of carbon filaments with Ni at tip is identified in the electronic enrichment of the active phase which reflects both in depressing the Bouduard reaction and the hydrocarbon decomposition activity which are considered the main responsible in the coke formation during reforming reactions [37]. As a consequence, the concentration of carbon on metal Ni surface never reach high value and carbon diffusion trough Ni particle is limited. In case of Rh/Al_2O_3 coke tends to encapsulate the particles (see Fig. 11a) while in the presence of oxygen in the reaction stream coke formation was drastically depressed and Rh particles appear to be completely free (Fig. 11b). TEM results were confirmed by carbon elementary analysis (CHNS) shown in Fig. 12: the coke formation rate significantly decreases in the presence of oxygen.

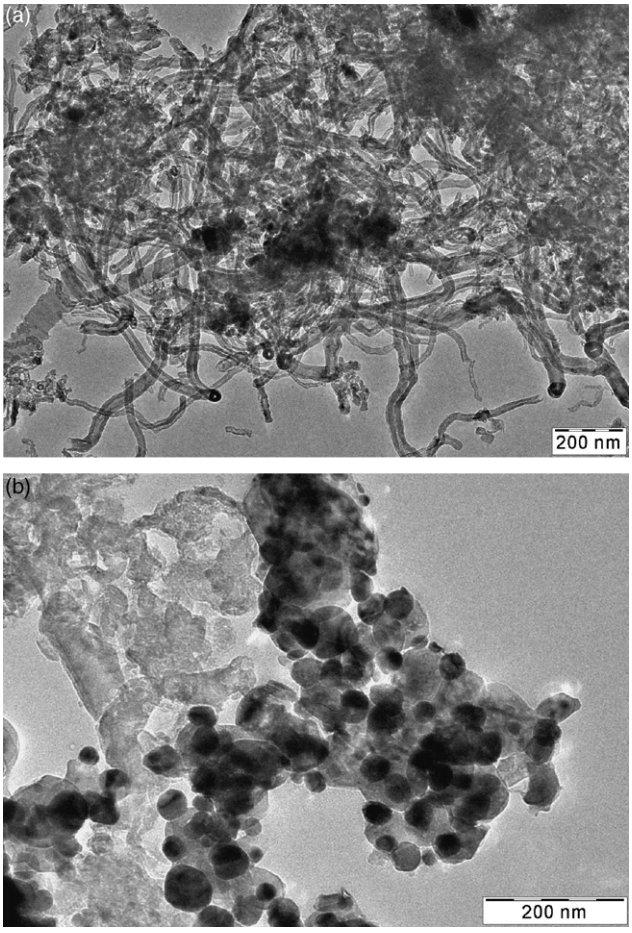

Fig. 10. Steam reforming of ethanol: TEM images of Ni/MgO aged catalysts: (a) bare Ni/MgO and (b) K doped Ni/MgO.

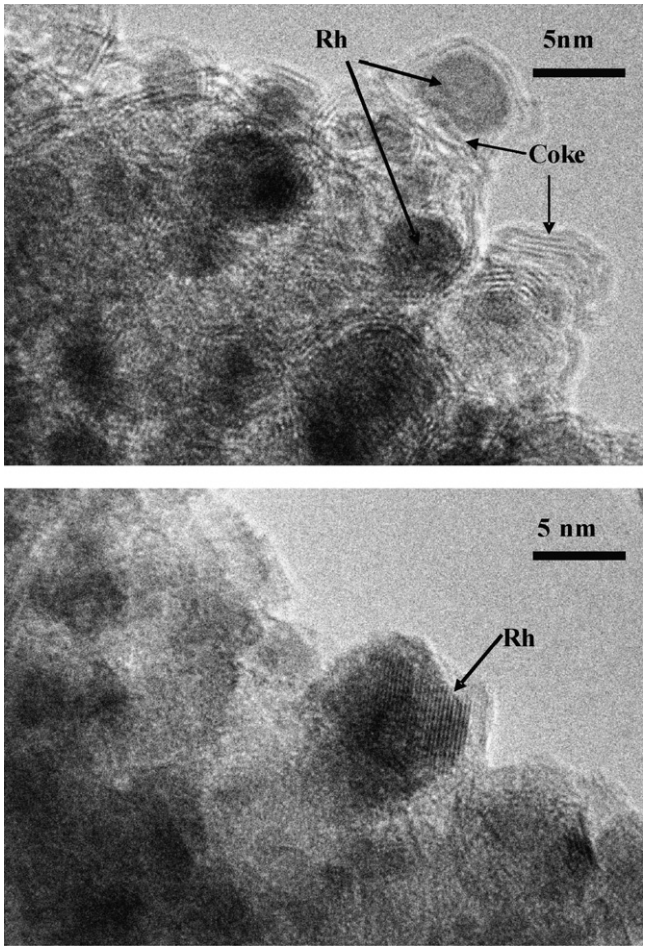

Fig. 11. Steam reforming of ethanol: TEM images of Rh/Al_2O_3 aged catalyst: (a) without oxygen in the fed gas and (b) with oxygen in the fed gas.

Different authors have observed significant benefits in performing steam reforming of ethanol in the presence of oxygen, both in terms of activity and catalysts stability [34]. Oxygen contributes to oxidize carbon residues formed during reaction maintaining free the metal active surface. Results obtained in our laboratory [38], reporting the behaviour of Ni/MgO and Ni/CeO_2 catalysts in reforming of bio-ethanol (see Figs. 13 and 14) in the presence of steam (SR) and oxygen (ATR)

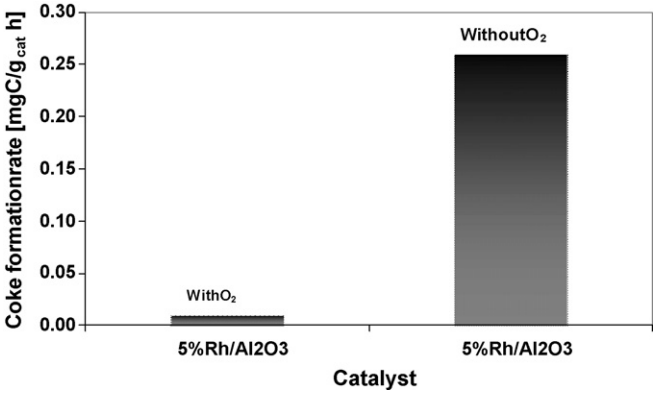

Fig. 12. Steam reforming of bio-ethanol over Rh/MgO catalyst: coke formation rate in the absence and in the presence of oxygen in the reaction stream.

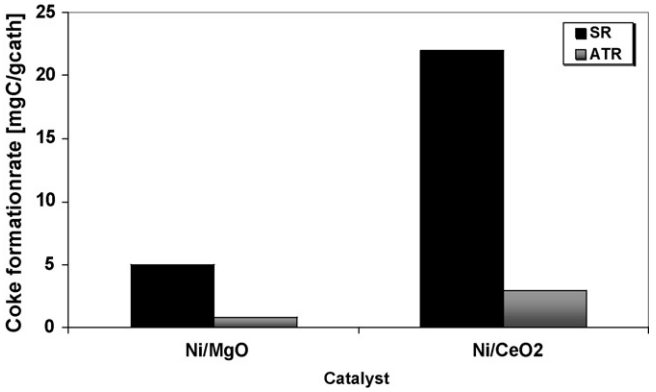

Fig. 13. Steam reforming of bio-ethanol: coke formation on Ni/MgO and Ni/CeO_2 catalysts in the steam and auto-thermal reforming.

have shown the fundamental role exerted by oxygen which, further to contribute to depress coke formation it enhances both catalyst activity and stability.

The steam reforming of ethanol at high temperature over noble metals has been also studied [39–43]. It is beyond doubt that Rh based catalysts shows the best performance both in terms of specific activity and catalyst stability. However, a perplexity remains concerning the extremely high activity in methanation reaction, which negatively reflects on the hydrogen productivity (CH_4 selectivity higher than 5–10% have been reported [44]). Pd resulted to be less active than Rh and in addition is not so active in methane conversion and this negatively affects the hydrogen productivity [45].

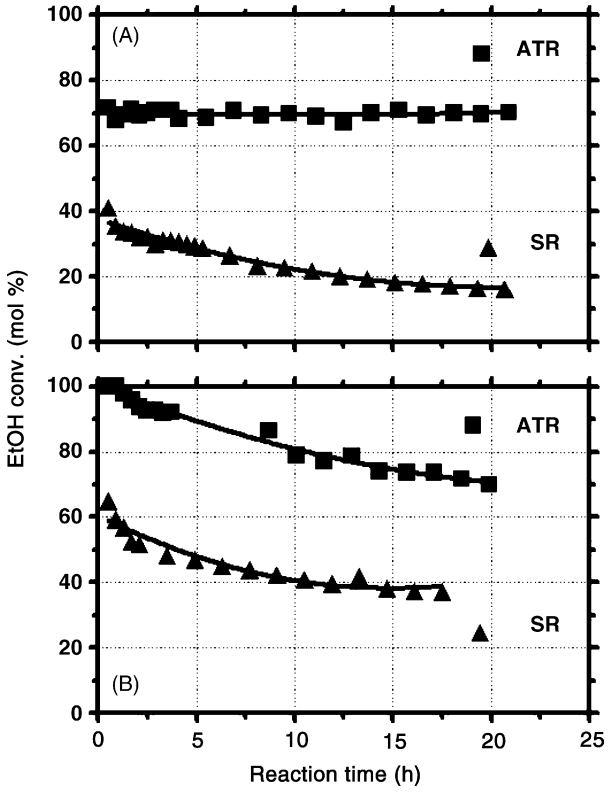

Fig. 14. EtOH conversion vs. reaction time on (A) Ni/CeO_2 and (B) Ni/MgO catalysts. A comparison between SR and ATR conditions: $T_R = 650\,^{\circ}C$; $GHSV = 40{,}000\,h^{-1}$.

Ru-containing catalysts supported on cordierite monolith has been recently proposed for the hydrogen production by partial oxidation of ethanol [45]. Catalyst seems to be enough stable but too high selectivity to CH_4, C_2H_4 and C_2H_6 were found.

7. Conclusions

- Bio-ethanol steam reforming appear to be very promising to produce hydrogen for MCFC application;
- MCFC electric performance using a hydrogen rich gas coming from reforming of bio-ethanol is very similar to that of MCFC fed with a conventional fuel;
- for a good thermal balance of the MCFC overall plant the high flow rate of steam in the reaction stream must careful computed;
- the ethanol steam reforming reaction mechanism in general evolves through the formation of acetaldehyde as first step. Acetaldehyde, further to be steam reformed, decomposes into methane and CO restraining so the hydrogen productivity to the conversion of methane by steam reforming;
- the metal sintering and the coke formation represent the main causes of deactivation of reforming catalyst;
- in IR-MCFC configuration further to consider the catalyst deactivation due to the metal sintering and coke formation, the deposition of vapour carbonates coming from electrolyte must also be considered;
- the presence of low amount of oxygen in the reaction stream positively affects both activity and stability of reforming catalyst mainly depressing the coke formation;
- Co/ZnO catalyst resulted to be a promising catalyst for the CO free H_2 production at low temperature;
- Ni/La_2O_3, Rh/MgO and K-Ni/MgO demonstrated to posses adequate properties to be used at high temperature in MCFC.

References

[1] S. Freni, J. Power Sources 94 (2001) 14–19.
[2] S. Cavallaro, S. Freni, J. Power Sources 76 (1998) 190–196.
[3] S. Freni, M. Aquino, E. Passalacqua, J. Power Sources 52 (1994) 41–47.
[4] S. Freni, S. Cavallaro, N. Mondello, L. Spadaro, F. Frusteri, J. Power Sources 108 (2002) 53–57.
[5] Y. Miyake, N. Nakanishi, T. Nakajima, Y. Itoh, T. Saitoh, A. Saiai, H. Yanaru, J. Power Sources 56 (1995) 11–17.
[6] S. Cavallaro, N. Mondello, S. Freni, J. Power Sources 102 (2001) 198–204.
[7] V. Galvita, G.L. Semin, V.D. Belyaev, V.A. Semikolenov, P. Tsiakaras, V.A. Sobyanin, React. Kinet. Catal. Lett. 71 (1) (2000) 143–152.
[8] S. Freni, G. Maggio, Int. J. Energy Res. 21 (1997) 253–264.
[9] S. Cavallaro, S. Freni, R. Cannistraci, M. Aquino, N. Giordano, J. Hydrogen Energy 17 (3) (1992) 181–186.
[10] R.J. Berger, E.B.H. Doesburg, J.G. van Ommen, J.R.H. Ross, App. Catal. A: Gen. 143 (1996) 343–365.
[11] E. Passalacqua, S. Freni, F. Barone, A. Patti, Mater. Lett. 29 (1996) 177–183.
[12] S. Freni, F. Barone, M. Puglisi, Int. J. Energy Res. 22 (1998) 17–31.
[13] D.A. Shores, J.R. Selman, E.T. Ong, Proc. Fuel Cell Semin., Phoenix 25–28 (1990) 294–297.
[14] H. Kansay, Y. Hayakawa, H. Ukai, S. Yajima, Denki Kagaku 64 (1996) 526–532.
[15] S. Cavallaro, Energy Fuels 14 (2000) 1195–1199.
[16] F. Frusteri, S. Freni, L. Spadaro, V. Chiodo, G. Bonura, S. Donato, S. Cavallaro, Catal. Commun. 5 (2004) 611–615.
[17] P.-Y. Sheng, G.A. Bowmaker, H. Idriss, Appl. Catal. A: Gen. 261 (2004) 171–181.
[18] A. Yee, S.J. Morrison, J. Scott, H. Idriss, J. Catal. 191 (2000) 30–45.
[19] J. Llorca, N. Homs, J. Sales, P.R. de la Piscina, J. Catal. 209 (2002) 306–317.
[20] J. Llorca, P.R. de la Piscina, J.-A. Dalmon, J. Sales, N. Homs, Appl. Catal. B: Environ. 43 (2003) 355–369.
[21] J. Llorca, N.J.-A. Homs, J. Sales, J.L.G. Fierro, P.R. de la Piscina, J. Catal. 323 (2004) 470–480.
[22] S. Freni, S. Cavallaro, N. Mondello, L. Spadaro, F. Frusteri, Catal. Commun. 4 (2003) 259–268.
[23] J. Sun, X.-P. Qiu, F. Wu, W.-T. Zhu, Int. J. Hydrogen Energy 30 (2005) 437–445.
[24] F. Mariño, G. Baronetti, M. Jobbagy, M. La borde, Appl. Catal. A: Gen. 238 (2003) 41–54.
[25] F. Mariño, M. Boveri, G. Baronetti, M. La borde, Int. J. Hydrogen Energy 26 (2001) 665–668.
[26] F. Mariño, M. Boveri, G. Baronetti, M. La borde, Int. J. Hydrogen Energy 29 (2004) 67–71.
[27] D. Srinivas, C.V.V. Satyanarayana, H.S. Potdar, P. Ratnasamy, Appl. Catal. A: Gen. 246 (2003) 323–334.
[28] P.-Y. Sheng, A. Yee, G.A. Bowmaker, H. Idriss, J. Catal. 208 (2002) 393–403.
[29] V.V. Galvita, G.L. Semin, V.D. Belyaev, V.A. Semikolenov, P. Tsiakaras, V.A. Sobyanin, Appl. Catal. A: Gen. 220 (2001) 123–127.
[30] M.A. Goula, S.K. Kontou, E.P. Tsiakaras, Appl. Catal. B: Environ. 49 (2004) 135–144.
[31] R.J. Berger, E.B.M. Doesburg, J.G. van Ommen, J.R.H. Ross, Appl. Catal. A: Gen. 143 (1996) 343–365.
[32] A.N. Fatsikosta, D.I. Kondarides, X.E. Verykios, Catal. Today 75 (2002) 145–155.
[33] F. Frusteri, S. Freni, V. Chiodo, L. Spadaro, O. Di Blasi, G. Bonura, S. Cavallaro, Appl. Catal. A: Gen. 270 (2004) 1–7.
[34] V. Fierro, V. Klouz, O. Akdim, C. Mirodatos, Catal. Today 75 (2002) 141–144.
[35] K.B.K. Teo, C. Singh, M. Chowalla, W.I. Milne, in: H. S. Nalwa (Ed.), Encyclopedia of Nanoscience and Nanotechnology, vol. X, pp. 1–22.
[36] K.O. De Chen, E. Christensen, Z. Ochoao-Fernàndez, B. Yu, N. Totdal, A. Latorre, A. Monzon, Holmen, J. Catal. 229 (2005) 82–96.
[37] F. Frusteri, S. Freni, V. Chiodo, L. Spadaro, G. Bonura, S. Cavallaro, J. Power Source 132 (2004) 139–144.
[38] F. Frusteri, S. Freni, V. Chiodo, S. Donato, G. Bonura, Int. J Hydrogen Energy 31 (15) (2006) 2193–2199.
[39] E. Vesselli, G. Comelli, R. Rosei, S. Freni, F. Frusteri, S. Cavallaro, Appl. Catal. A: Gen. 281 (2005) 139–147.
[40] S. Cavallaro, V. Chiodo, S. Freni, N. Mondello, F. Frusteri, Appl. Catal. A: Gen. 249 (2003) 119–128.
[41] J.P. Breen, R. Burch, H.M. Coleman, Appl. Catal. B: Environ. 39 (2002) 65–74.
[42] V.V. Galvita, V.D. Belyaev, V.A. Semikolenov, P. Tsiakaras, A. Frumin, V.A. Sobyanin, React. Kinet. Catal. Lett. 76 (2) (2002) 343–351.
[43] F. Auprêtre, C. Descorme, D. Duprez, Catal. Commun. 3 (2002) 263–267.
[44] D.K. Liguras, D.I. Kondarides, X.E. Verykios, Appl. Catal. B: Environ. 43 (2003) 245–354.
[45] D.K. Liguras, K. Goundani, X.E. Verykios, Int. J. Hydrogen Energy 29 (2004) 419–427.